Transient reflection spectra in topological nanocrystals of Bi_2Se_3, Bi_2Te_3, Bi_2Te_2Se

Faizan Ahmad[1], Rashmi Singh[1], Rachana Kumar[2*], Mukesh Jewariya[2, 4], Chandra Shekhar[3], Naresh Kumar[5], Pramod Kumar[1*]

[1]*Spintronics and Magnetic Materials Laboratory: Department of Applied Sciences, IIIT-Allahabad, 211012, India*
[2]*CSIR-National Physical Laboratory: New Delhi, 110012, India*
[3]*Max Planck Institute for Chemicals Physics of Solid: Nöthnitzer Straße, 40, 01187 Dresden, Germany*
[4]*Center for Quantum-Beam-based Radiation Research: Korea Atomic Energy Research Institute (KAERI), Korea*
[5]*Department of Physics, Motilal Nehru National Institute of Technology Allahabad 211004, India*

[*]Corresponding author, Tel: (+91) 0532-2922202; E-mail: pkumar@iiita.ac.in; rachanak@nplindia.org

Received: 01 May 2016, Revised: 09 August 2016 and Accepted: 30 October 2016

DOI: 10.5185/amlett.2017.6898
www.vbripress.com/aml

Abstract

The wavelength and time delay dependent reflection spectra of nano crystals Bi_2Se_3, Bi_2Te_3 and Bi_2Te_2Se were studied for ultrafast dynamics, using pump and probe spectroscopy. We observed only one transient peak for Bi_2Se_3 below 600nm, which decreases linearly with time delay. Three transient sharp peaks were observed for Bi_2Te_3 for wavelength dependent graph, which reveals about the ultrafast dynamics of charge carrier. We also observed oscillations in Bi_2Se_3 crystal above 600 nm which was absent in Bi_2Te_3 sample. Bi_2Te_2Se showed a single transient spectrum peak at 482 nm with the highest peak for 103ps time delay. The curve fitted Time resolve (TR) trace for both Bi_2Se_3 and Bi_2Te_3 crystals at 492 nm wavelength, revealed almost the same results for rise and decay time.

Keywords: Ultrafast, topological, transient, spectra, femtosecond.

Introduction

Topological insulators (TI) are a new class of insulating materials that conducts electricity through special surface electronics states [**1**]. The surface state of TI is topologically protected by the time reversal symmetry [**2-3**] which makes the electrons "dissipation less" [**4**] in case of non-magnetic impurity, making the bulk insulated, not being adiabatically connected to the surface. The properties of the topological materials are explained by two features of quantum mechanics: the reversal of time, and the spin-orbit coupling occurring in heavy elements such as Bismuth and Mercury. Some of the 3-dimensional materials exhibiting these properties, having metallic surface bands, and forming a Dirac-cone are Bi_2Se_3, Sb_2Te_3 and Bi_2Te_3. This property makes them favorable for new generation of electronic devices. But for such realization to be practical, an insight into dynamical response and further knowledge of electronic states are required. Due to the fact that Dirac-cone is a surface feature, it becomes essential to determine the interband scattering range i.e. the distance over which the surface band exchange carriers with the bulk. Angle resolved photoemission spectroscopy (ARPES) [**5, 6, 7**] and time resolved photoemission spectroscopy (TrARPES) are the two effective methods to probe the metallic and two dimensional (2D) Dirac surface states (SS) of TIs. They use photoelectric effect i.e. high energy photons are shone onto the sample surface ejecting the electrons. By analyzing the energy, spin and momentum of these electrons, the electronic structure and spin polarization can be directly measured. But these techniques are limited due to their sensitivity to SS and bulk atoms, therefore we need a novel solution that is insensitive to the sample surface and can individually probe the bulk and the surface state. The advent of optical pump-probe mid infrared (mid-IR) spectroscopy provides the answer to the problem, which is a bulk sensitive technique and is used to explore the non-equilibrium dynamics of the TIs. By using multiple femtosecond laser pulse [**28**], transitions involved between different states of the molecular system are probed and information about various dynamical process are extracted which are otherwise hidden by macroscopic inhomogeneous broadening. Femtosecond pump-probe spectroscopy [**28**] enables to follow in, real time vibrations coupled to electronic transitions. Being excited by pulse shorter than the vibrational period, vibrational coherence is induced both in the ground state and excited electronics states which provides information on excited state nuclear dynamics. It also allows us to probe the fundamental relaxation process directly within conduction band and Dirac-cone, distinguishing the surface and the bulk dynamics. The information about different molecular dynamics such as de-coherence times,

vibrational relaxation times, population lifetimes and coherence coupling can thus be extracted. In addition, time domain vibrational spectroscopy evades the difficulty faced in Raman spectroscopy of discriminating the low frequency modes against the laser line. It has also been effectively employed to fabricate various optical elements such as optical waveguide, couplers, gratings, photon crystals and other functional optoelectronic devices [**8-13**].

In our present work, we have prepared single nano crystals of Bi_2Se_3, Bi_2Te_3 and Bi_2Te_2Se, and carried out the optical pump-probe spectroscopy using femtosecond laser pulse which gives useful information about the surface states of TIs. Reflection spectra results were studied and correlated for all the crystals with the objective of studying the ultrafast dynamics of the charge carriers in different surface energy states.

Experimental

Materials/ chemicals details

We have used Bismuth(ш) and Selenium with purity of 99.999% (metal basis), Tellurium with 99.98% purity (metal basis). All the chemicals were brought from Alfa Aesar.

Material synthesis

Single nano size crystal of Bi_2Se_3 [**14**], Bi_2Te_3 [**16**] and Bi_2Te_2Se [**15**] were grown by self-flux method [**16**] in the furnace, we obtained the optimal preparation conditions by adjusting the parameters of heat treatment, single phase for the crystals were confirmed by XRD.

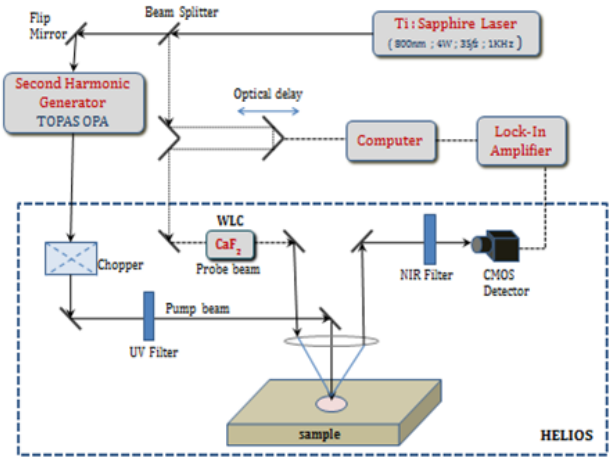

Fig. 1. Experimental set up for optical pump probe spectroscopy.

Characterizations

To perform ultrafast optical pump-probe spectroscopy, a train of optical pulses from a Ti: Sapphire laser amplifier (35 fs, 4 mJ/pulse, 1 KHz, 800 nm) was split into two beams with a beam splitter as shown in **Fig. 1.** One with high intensity was used as a pump and an optical parametric amplifier (TOPAS, Light Conversion) was employed to vary the wavelength of this pump beam from 190 nm to 2600 nm. The other beam with weak intensity, was propagated through a CaF_2 crystal to generate white light continuum (WLC) covering the whole spectrum of visible light to be used as a probe beam. The probe beam was optically delayed with respect to pump beam using a computer-controlled delay stage. The intrinsic temporal resolution of delay stage was 7 fs. Here we have performed ultrafast pump-probe spectroscopy using 490-550 nm pump beam at normal incidence and the changes in absorption was detected by using a gated-CMOS detector. The pump pulse power was intentionally kept low (35 mW) for all the measurements to avoid any damage on TI surfaces. The time resolved study was performed using HELIOS (Ultrafast systems) spectrometer [**17-23]**.

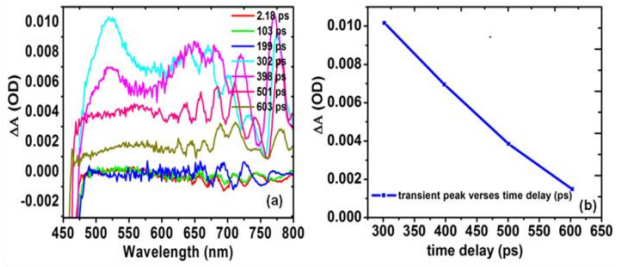

Fig. 2. (a) Reflection spectra showing amplitude variation ΔA verses wavelength (nm) of the probe for Bi_2Se_3 (b) Peak variation for Bi_2Se_3 verses time delay (ps) between the pump and probe as observed from transient spectra.

Results and discussion

Results for single crystal Bi_2Se_3, Bi_2Te_3 and Bi_2Te_2Se were obtained with reflection spectra, showing the amplitude change v/s wavelength of probe beam for different time delays (ps). For Bi_2Se_3, an increase in amplitude was observed for shorter wavelength range (nm) of the probe **[Fig. 2a].** High amplitude reflection was observed with large rise time for probe delay (302-603 ps) showing the exited state absorption [**24**] in the form of positive ΔA spectrum. Maximum absorption was observed at 302 ps delay. The oscillations were clearly visible at higher wavelength range (600-800 nm) for the Bi_2Se_3 crystal. These oscillations became less prominent for smaller time delay range (199 -2.18 ps) as compared to higher delay range (302-603 ps) between the pump and probe. Major oscillations were observed beyond 620 nm (below Energy=1.99 eV). The oscillations had highest value at 398 ps time delay at 770 nm (Energy=1.61 eV) probe wavelength. The transient peak spectra for Bi_2Se_3 shows a linear decreasing behavior with time delay between the pump and the probe **(Fig. 2b)** with the highest peak value at 302 ps. The oscillations may be possible due to consecutive, excited state absorption and stimulated emission for that excited state [**24**], it may be due to the bulk state electrons moving to the surface. The higher wavelength oscillations correspond to the small transitions that are observed due to the movement of electron into different states on the surfaces of the Bi_2Se_3 crystal.

Fig. 3 shows the reflection spectra of Bi_2Te_3 crystal obtained by the pump probe spectroscopy. Positive transient spectra peak P1 (**Fig. 3**) was obtained at 409 nm (Energy=3.03 eV) which have greater than the pump intensity of 2.53 eV (490 nm), indicating excited state

absorption [**24**]. It is due to optically allowed transition from the excited state to higher excited state [**24**].

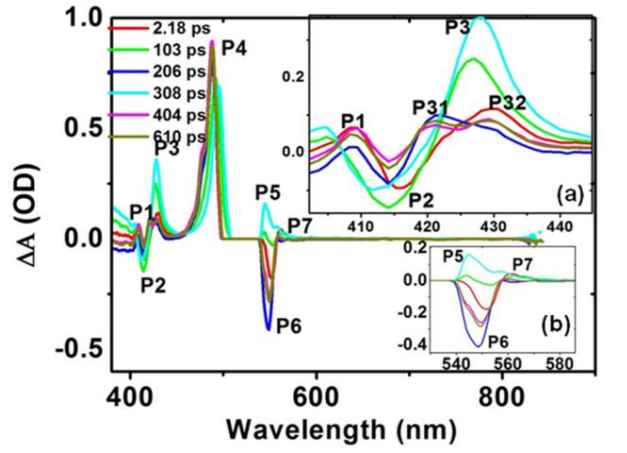

Fig. 3. Reflection spectra of Bi_2Te_3 showing reflectivity variation ΔA verses wavelength (nm) of probe for different time delays between pump and the probe. Inset (a) shows enlarged image for the spectra peaks P1, P2 & P3 and (b) shows the enlarged spectra peaks P5, P6 & P7.

Second transient spectra peak P3 was observed at 427 nm wavelength for two probe delays (103 nm, 308 nm), whereas for other delays two spectra peaks were observed at 421 nm and 429 nm as revealed by the inset **(Fig. 3c)**. A major peak P4 obtained at 490 nm (2.53 eV) shows the pump peak. The negative spectra peak P2, revealing the ground state bleach [**24**], was obtained at 413 nm (3.00 eV) that shows less absorption due to less electrons in the ground state, with some stroke shifted spectrum representing the stimulated emission [**24**]. Another transient spectra peak at P5 **(Fig. 3 a & b)** was obtained at 544 nm for two time delays (103 ps, 308 ps). For all other time delays, ground bleach with stimulated emission was observed with stroke shifted spectrums [**24**]. One more transient spectra peak P7 was observed at 560 nm showing the excited state absorption [**24**] to higher energy states. No oscillations were observed in Bi_2Te_3 single crystal spectra unlike Bi_2Se_3, where oscillations were clearly visible at higher values of the wavelength.

Fig. 4 shows the Transient spectra results obtained for Bi_2Te_2Se crystals. P1 & P3 were two negative spectra peaks obtained at 414 nm and 486 nm, respectively, which showed the ground state bleach [**24**]. The negative peak might be the result of stimulated emission. Stroke shifted spectrum [**24**] were obtained for both the negative peaks as observed before. The major negative peak observed at 547 nm (2.26 eV) wavelength shows the pump peak. The transient spectra peak P2 was observed at 482 nm (2.57 eV) which was attributed due to the excited state absorption of the photon and the movement of charge carriers [**24**] to higher energy states. Here the excited state population may be affected since the probe energy is higher than the pump energy. **Fig. 4c** in the inset shows the transient spectra peak variation of Bi_2Te_2Se for the peak P2 **(Fig. 4a & b)**.

The peak value increases upto 103 ps time delay and then decreases upto 199 ps and then again increases with further increase in the time delay between the pump and probe (Inset of **Fig. 4**). The maximum peak value was obtained at 103 ps time delay as depicted by the blue graph (**Fig. 4a**).

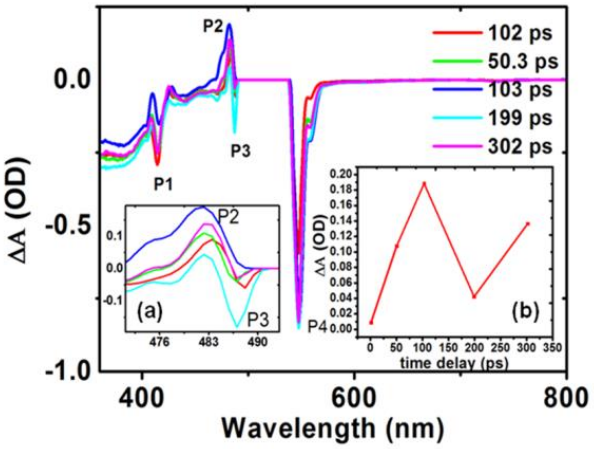

Fig. 4. Reflection spectra of Bi_2Te_2Se at different time delays between the pump and the probe. Inset (a) shows the enlarged image for the transient spectra peak P2 and negative spectra peak P3 and Inset (c) shows the transient spectra peak variation of P2 with respect to the time delay between the pump and the probe.

As compared to the Bi_2Te_3 an additional transient spectra peak at 482 nm was observed which may be due to the addition of another Se atom in place of Te [**25**]. We observed that the highest transient spectra peak for Bi_2Te_2Se at 103 ps **(Fig. 4a)** as compared to that of the Bi_2Te_3 where the highest transient spectra peak was obtained at 308 ps **(Fig. 3)**. This implies that the excited state absorption for Bi_2Te_2Se takes place earlier than that of Bi_2Te_3.

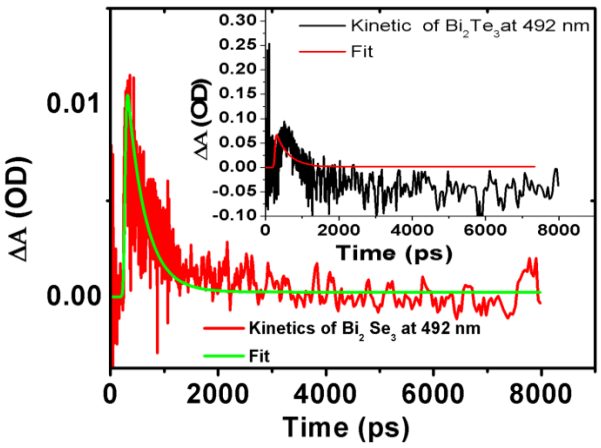

Fig. 5. (a) TR trace showing the amplitude variation as a function of time delay (ps) at 492 nm wavelength for Bi_2Se_3 crystal with the green curve showing the best fit exponential curve. Inset shows the TR trace for Bi_2Te_3 at 492 nm crystal with the red curve showing the best fit exponential curve.

Fig. 5 shows the TR trace for reflectivity dynamics of the grown Bi_2Se_3 crystal as a function of time for different range of the probe wavelength (nm). Maximum positive reflectivity was observed for time delay (220-2500 ps) showing the maximum absorption and then the amplitude decays exponentially. The amplitude decreases with the decrease in frequency of the probe. The exponential fitting was done for one rise time (t_r) and two decay time

constant (t_{d1}, t_{d2}) for both the crystals, using two exponential decay functions. **Fig. 5** shows the curve fitting for 492 nm wavelength. The rise time was found to be t_r=268 ps with instrument response function t_0 (IRF)= 47.37 ps. The rise time in Bi_2Se_3 (~ 200 ps) was much longer than expected for typical semiconductors and metals (~ 300 fs) [**26**] .This time scale corresponds to the delayed thermalization of carriers via electron-electron interactions. The two delay times obtained were t_{d1}=334.7 ps and t_{d2}=4.053 ns. The shortest delay t_{d2}=4.053 ns was assosiated with electron-phonon relaxation, whereas the longer delay t_{d1}=334.7 ps was assosiated with the charge seperation [**27**] or thermal effects [**28**]. **Fig. 5b** in the inset shows the TR spectra between the reflectivity and the time delay for Bi_2Te_3 nano crystal. It shows negative amplitude for 549 nm probe wavelength for different time delay range (ps), which shows a highly correlated electron system as observed earlier [**29**]. Short amplitude oscillations were observed for the wavelength range (408–561 nm) of the probe at varying time delay range (ps). The curve fitting [Inset of **Fig. 5**] for Bi_2Te_3 at 492 nm wavelength resulted in a rise time of t_r=223.7 ps with the instrument response function t_0=33.21 ps and the two delay time obtained were t_{d1}=293 ps and t_{d2}=3.03 ns. We see no major differences in the range of rise and the delay time except the negative amplitude behavior for 549 nm range. The shortest delay t_{d2}=3.03 ns was assosiated with the electron-phonon relaxation, whereas the long delay t_{d1}=293 ps was assosiated with the charge seperation [**27**] or thermal effects [**28**] due to charge carriers.The transient signal for Bi_2Te_2Se crystal was weak so it was not possible to fit the exponential curve for it.

Conclusion

The wavelength and the time delay dependent characteristics of reflectivity spectra of these crystals were studied separately. The oscillations were clearly visible for Bi_2Se_3 above 600 nm wavelength and its transient spectra peak, decreases linearly with the time delay, with the highest peak for 302 ps delay. The Bi_2Te_3 crystal showed transient spectra peak at 409 nm, 427 nm and 544 nm wavelength, with the highest peak amplitude for 308 ps time delay. The Bi_2Te_2Se crystal showed the transient spectra peak at 482 nm, with the highest peak for 103 ps time delay. TR trace for both Bi_2 Se_3 and Bi_2 Te_3 crystals were analysed and the curve fitting for 492 nm wavelengths revealed almost the same result for rise and decay time. The transient signals for Bi_2Te_2Se crystal were weak so exponential curve fitting was not possible.

Acknowledgements

One of the authors (Pramod Kumar) thanks DST, Govt. of India for proving financial support for this work.

Author's contributions

All authors contributed equally towards completing the project and I like to thanks for their valuable dicussions.

References

1. Moore, J. E.; Nature., **2010**, 194,464 **DOI:** 10.1038/nature08916
2. Murakami, S. ; New J. Phys., **2007**, 9, 356 **DOI:** 10.1088/1367-2630/9/9/356
3. Hasan, M. Z.; Kane, C. L.; Rev. Mod. Phys.,**2010**, 82, 3045 **DOI:** 10.1103/RevModPhys.82.3045
4. Moore, J. E.; Mahmood, F.; Chan, C-K.; Alpichshew, Z.; Gardner, D.; Lee, Y.; Lee, P. A.; Gedik, N.; Nature Physics., **2009**, 460, 1090 **DOI:** 10.1038/nphys3609
5. Chen, Y. L.; Analytis, J. G.; Chu, J.H.; Liu, Z. K.; Mo, S.K.; Qi, X. L.; Zhang, H. J.; Lu, D. H. ; Dai, X.; Fang, Z.; Zhang, S. C.; Fisher, I. R.; Hussain, Z.; Shen, Z.X.; Science., **2009**, 325, 178 **DOI:** 10.1126/science.1173034
6. Sobota, J. A.; Yang, S.; Analytis, J. G.; Chen, Y. L.; Fisher, I. R.; Kirchmann, P. S.; Shen, Z.X.; Phys. Rev. Lett., **2012**, 108, 117403 **DOI:** 10.1103/PhysRevLett.108.117403
7. Wang, Y. H.; Hsieh, D.; Sie, E. J.; Steinberg, H.; Gardner, D. R.; Lee, Y. S.; Phys. Rev. Lett.**, 2012**, 109**,** 127401 **DOI:** 10.1103/PhysRevLett.109.127401
8. Engel, S.; Knoth, K.; Huhne, R. ; Schultz, L.; Holzapfel, B.; Supercond. Sci. Technol., **2005**, 18, 1385 **DOI:** 10.1088/0953-2048/18/10/024
9. Solovyov, V.F.; Develos-Bagarinao, K.; Li, Q.; Qing, J.; Zhou, J.; Supercond. Sci. Technol., **2010**, 23, 014008 **DOI:** 10.1088/0953-2048/23/1/014008
10. Xiong, J.; Chen, Y.; Qiu, Y.; Tao, B.; Qin, W.; Cui, J.;Tang, Li, Y.; Supercond. Sci. Technol., **2006**, 19, 1068 **DOI:** 10.1088/0953-2048/19/10/014
11. Singh, R. P.; Choi, J. W.; Tiwari, A.; Pandey, A. C., *Intelligent Nanomaterials: Processes, Properties, and Applications*, **2012**, 741.
12. Singh, P.;Srivatsa, K. M. K.; Das, S.; Adv. Mater. Lett., **2015**, 6(5), 436 **DOI:** 10.5185/amlett.2015.5884
13. Dutta, P.; Rathi M.; Yao, Y.; Gao, Y.;Majkic, G.; Iliev, M.; Martinez, J.; Holzapfel, B.;. Selvamanickam, V.; RSC Adv., **2014**, 4, 21042 **DOI:** 10.1002/adma.200500040
14. ViolBarbosa, C.E.;Shekhar, C.; Yan, B.; Ouardi, S.; Ikenagar,E.; Fecher, G.H.; Felser, C.; Physical Review B., **2013**, 88(19),195128. **DOI:** 10.1103/PhysRevB.88.195128
15. Shekhar, C.;ViolBarbosa, C. E.; Yan, B.; Ochnelle,W.; Fecher, G.H.; Felser, C.; Physical Review B., **2014**, 90 (16),1 **DOI:** 10.1103/PhysRevB.90.165140
16. Chen, P.; Zhou, D.; Li, P.; et al. J. Mod. Transport., 2014 **DOI:** 10.1007/s40534-014-0037-z
17. Cheng, H. L.; Suo, Y.; Zhao, M .; Gao, M. ;Y. H. Zhu, Y. H. ; Wang, R. ; Liu, M. ; Ma, L.;. Zhou, M. L.; Physica C., **2011**, 471, 982 **DOI:** 10.1016/j.physc.2011.05.105
18. Aytug, T.; Paranthaman, M.; Kang, S.; Zhai, Y. S.; Leonard, K. J.; Vallet, C. E.; Sathyamurthy, S.; Christen, H. M.; Goyal, A.; Christen, D. K.;IEEE Trans. Appl. Supercond., **2003**, 13, 2661 **DOI:** 10.1088/0953-2048/17/5/050
19. Paranthaman M. P.; Qiu, X.; List, F. A.; Kim, K.; Zhang, Y.; Li, X.; Sathyamurthy, S.;. Thieme, C.; Rupich, M. W.; IEEE Trans. Appl. Supercond., **2011**, 21, 3059 **DOI:** 10.1109/TASC.2010.2092731
20. Zhao, Y.; Grivel, J. C.; CrystEngComm., **2013**, 15, 3816 **DOI:** 10.1039/C3CE40245B
21. Lee, H-G.; Lee, Y. M.; Shin, H. S.; Kim, C. –J.; Hong, G.–W.; Mater. Sci. Eng. B., **2002**, 90, 20 **DOI:** 10.1016/S0921-5107(01)00940-0
22. Wang, R. P.; Zhou, Y. L.; Pan, S. H.; He, M.; Lu, H. B.; Chen, Z. H. ; Yang, G. Z.; Liu, C. F.; Wu, X. ; Wang, F. Y.; Feng, Y.; Zhang, P. X.; Wu, X. Z.; Zhou, L.; Physica C., **2000**, 337, 87 **DOI:** 10.1016/S0921-4534(00)00062-9
23. Lee, J. B.; Park, S. K.; Kim, B. J.; Lee, H. J.; Kim, S. S.; Moon, S. H.; Lee , H. G.; Hong, G. W.; Physica C., **2011**, 471, 978 **DOI:** 10.1016/j.physc.2011.05.104
24. Xiong, J.; Chen, Y.; Qiu, Y.; Tao, B.; Qin, W.; Cui, X.; Li, Y.; J. Mater. Sci. Technol., **2007**, 23, 457 **DOI:** 10.3321/j.issn:1005-0302.2007.04.003
25. Hsieh, D.; Mahmood, F.; McIver, J. W.; Gardner, D. R.; Lee, Y. S.; Gedik, N.; Phys. Rev. Lett., **2011**, 107, 077401

DOI: 10.1103/PhysRevLett.107.077401
26. Rast, S.; Schneider, M. L.; Onellion, M.; Zeng, X. H.; Si, W.; Xi, X. X.; Abrecht, M.; Ariosa, D.; D. Pavuna, Y. H. Ren, G. Lüpke, and I. Perakis, Phys.Rev. B., **2001**, 64, 214505
DOI: 10.1103/PhysRevB.64.214505
27. Glinka, Y. D.; Tolk, N. H.; Liu, X.; Sasaki, Y.; Furdyna, J. K.; J. App Phys., **2008**, 103, 043708
DOI: 10.1063/1.2840139
28. Johnson, J. A.; Maznev, A. A.; Bulsara, M. T.; Fitzgerald, E. A.;.Harman, T. C.; Calawa, S.; Vineis, C. J.; Turner, G.; Nelson, K. A.; J. Appl.Phys., **2012**, 111, 023503
DOI: 10.1063/1.3675467
29. Hannaford, Peter (Ed.); Femtosecond Laser Spectroscopy; Springer: US, **2005.**
DOI: 10.1007/b101192